Unusual Ca^{2+}-Calmodulin Binding Interactions of the Microtubule-Associated Protein F-STOP[†,‡]

Denis Bouvier,[§] Cécile Vanhaverbeke,[§] Jean-Pierre Simorre,[§] Gérard J. Arlaud,[||] Isabelle Bally,[||] Vincent Forge,[⊥] Robert L. Margolis,[#] Pierre Gans,*[,§] and Jean-Philippe Kleman[#]

Laboratoire des Protéines du Cytosquelette, Laboratoire de Résonance Magnétique Nucléaire, Laboratoire d'Enzymologie Moléculaire, Institut de Biologie Structurale J-P Ebel (UMR CNRS 5075), 41 rue Jules Horowitz, 38027 Grenoble Cedex 1, France, and Laboratoire de Biophysique Moléculaire et Cellulaire (UMR CNRS 5090), Département Réponse et Dynamique Cellulaire, CEA-Grenoble, 17 rue des Martyrs, 38054 Grenoble Cedex 1, France

Received May 7, 2003; Revised Manuscript Received August 6, 2003

ABSTRACT: F-STOP is a microtubule-associated protein that stabilizes microtubules in a calmodulin (CaM)-dependent manner. All members of the stable tubule only polypeptide (STOP) family have a central domain that contains nearly identical multiple repeats, and a CaM binding motif is present in multiple copies within this domain. We present here an analysis of this CaM binding interaction and find that it is highly unusual in nature. For this work, we synthesized two model peptides of a single STOP central repeat motif and analyzed their binding to CaM by fluorescence, circular dichroism, infrared and NMR spectroscopy. Both peptides bind to CaM with an affinity of 4 μM, similar to that of the native protein. Results indicate that the peptides bind CaM in an atypical manner. Binding is highly dependent on the concentration of cations, indicating that it is to some extent electrostatic. Further, IR and CD analysis shows that, in contrast to typical CaM binding reactions, CaM does not change in helical structure on binding. NMR mapping confirms that CaM remains in extended conformation on binding a single STOP peptide. Binding of a single peptide to CaM occurs principally in the CaM C-terminal region, and the C-terminal domain of CaM effectively competes for STOP binding. Our results establish that CaM binds STOP in an unusual manner, involving mainly the C-terminus of CaM, thus leaving CaM potentially accessible for another binding partner at the N-terminus. This intriguing possibility could be of physiological importance in F-STOP mediated CaM regulation of microtubule dynamics or stability, specifically during mitosis where CaM and STOP colocalize.

Microtubules are ubiquitous components of the cytoskeleton in eucaryotic cells. They are intrinsically labile polymers of tubulin, physiologically stabilized by the association with microtubule-associated proteins (MAPs)[1] (*1*). Among the MAPs, stable tubule only polypeptide (STOP) family members have the unique capacity to prevent in vitro dissociation of microtubules after exposure to cold temperature, dilution, or microtubule depolymerizing drugs (*2*, *3*). STOP protein variants are produced from a single gene by alternate splicing (*4*, *5*). The short F-STOP splice variant is expressed in cycling cells. E- and N-STOP are longer forms, respectively expressed during embryogenesis or in neurons. Physiological roles of STOPs are not at present clearly understood, but STOP inhibition in cultured neuronal cells impairs neuronal differentiation (*6*). Furthermore, knockout mice for STOPs exhibit synaptic defects associated with a severe behavioral phenotype (*7*), suggesting that STOP might be implicated in synaptic functions. F-STOP is physiologically associated with specific microtubules of the mitotic spindle (*5*), and is thus believed to play a role in cell cycle progression during mitosis.

CaM is known to bind STOP and to regulate its microtubule stabilizing capacity in a calcium-dependent manner (*8*, *9*). CaM is a major sensor of cytoplasmic Ca^{2+} concentration, and is implicated in hundreds of cellular processes through calcium specific binding to effectors (*10*). The diverse STOP variants are all implicated or colocalized with CaM, in nerve terminals and in the mitotic spindle (*11*, *12*),

[†] This work was supported by the Centre National de la Recherche Scientifique, the Commissariat à l'Energie Atomique and the University Joseph Fourier.

[‡] Chemical shift assignments of the backbone atoms of VU-1 calmodulin and of calmodulin in the complex VU-1 calmodulin/STP23 have been deposited in the BioMagResBank (accession numbers 5893 and 5896, respectively).

* To whom correspondence should be addressed: E-mail: pierre.gans@ibs.fr. Tel: (33) 4 38 78 57 98. Fax: (33) 4 38 78 54 94.

[#] Laboratoire des Protéines du Cytosquelette, Institut de Biologie Structurale J-P Ebel (UMR CNRS 5075).

[§] Laboratoire de Résonance Magnétique Nucléaire, Institut de Biologie Structurale J-P Ebel (UMR CNRS 5075).

[||] Laboratoire d'Enzymologie Moléculaire, Institut de Biologie Structurale J-P Ebel (UMR CNRS 5075).

[⊥] Laboratoire de Biophysique Moléculaire et Cellulaire (UMR CNRS 5090), Département Réponse et Dynamique Cellulaire, CEA-Grenoble.

[1] Abbreviations: CaM, calmodulin; TR2C, C-terminal domain of calmodulin deletion mutant; STOP, stable tubule only polypeptide; N-STOP, neuronal form of STOP; F-STOP, fibroblastic form of STOP; STP23, STOP 23-mer peptide (Mc motif); STP42, STOP 42-mer peptide (repeat unit); NATA, *N*-acetyl-L-tryptophan amide; SAXS, small-angle X-ray scattering; nOe, nuclear Overhauser effect; bHLH, basic helix−loop−helix; MARCKS, myristoylated alanine-rich C kinase substrate; SEF2-1mp, SL3 enhancer factor 2-1 mimicking factor; M13, CaM-binding domain of myosin-light chain kinase; C20W, N-terminal portion of the CaM-binding domain of the plasma membrane pump; TFP, trifluoroperazine; W-7, *N*-(6-aminohexyl)-5-chloro-1-naphthalenesulfonamide.

10.1021/bi034746w CCC: $25.00
Published on Web 09/13/2003

where CaM has been implicated in chromosome segregation (*13*). CaM activation is also known to be essential for mitotic progression (*14*, *15*). These observations suggest a physiological role for CaM/STOP binding in various cell processes.

A recent study of STOP sequence properties using immobilized-peptide array revealed that multiple putative CaM binding motifs are present on STOP, and overlap with the microtubule binding sequences (*16*). The short splicing variant, F-STOP, exhibits one CaM/microtubule Mn binding motif and four Mc motifs, occurring once in each of the four conserved repeats in the central region. Bosc et al. (*16*) showed that only F-STOP constructs containing Mc repeats were retained on column-immobilized CaM, signifying that Ca^{2+}-CaM interaction with F-STOP is restricted to the Mc motifs present in its central repeated region. Sequence comparison showed that these motifs are not related to conventional CaM-binding motifs (*17*). Taken together, these observations suggest an unusual binding interaction between CaM and the F-STOP repeated central region.

Several unusual modes of interaction between CaM and its binding partners have been reported (*18*−*25*). However, none of these complexes, as described in Discussion, is representative of the binding mode of STOP. We wanted to understand the unique binding interaction between CaM and F-STOP. To gain structural knowledge on the complex formed between F-STOP and CaM, we decided to study their mode of interaction using a simplified peptide model. We have thus synthesized peptides corresponding either to the element within the repeat that contains the CaM/microtubule Mc binding motif (STP23), as described by Bosc et al. (*16*), or to the full-length repeat (STP42). We show that, in solution, these peptides bind to CaM in a calcium-dependent manner and that binding occurs in the C-terminal domain of CaM. Structural changes that are typical for CaM binding do not occur in the reaction between CaM and STOP. Our results thus demonstrate a unique mode of CaM binding, with potential physiological consequences.

EXPERIMENTAL PROCEDURES

Peptide Synthesis. The 23-mer peptide (STP23, rat sequence from EMBL NM_017204) corresponding to the consensus Mc motif (*16*), QRDTRRKAGPAWMVTRTEGHEEK was obtained commercially (Eurogentec France S. A.). The 42-mer peptide corresponding to a single repeat (STP42, mouse sequence from EMBL NM_010837) AQSQTQEGGPAAGKASGADQRDTRRKAGPAWMVTRSEGHEEK was synthesized chemically (Applied Biosystems 430A automated synthesizer). The *tert*-butyloxycarbonyl group was used for protection of the N-*a*-amino terminus of all amino acids, and synthesis was carried out on a phenylacetamidomethyl resin. Protecting groups for relevant amino acid side chains were as follows: R, mesitylene sulfonyl; D, cyclohexyl; E, benzyl; H, 2,4-dinitrophenyl; K, 2-chlorobenzyl oxycarbonyl; S and T, benzyl; W, formyl. All couplings were performed by the dicyclohexylcarbodiimide/1-hydroxybenzotriazole method, using *N*-methyl pyrrolidone and dimethyl sulfoxide as coupling solvents, according to the protocol recommended by Applied Biosystems. All amino acids except glycine were double-coupled, and amino groups left unreacted at the end of each coupling cycle were capped with acetic anhydride. Deprotection and cleavage of the peptide from the resin were achieved by HF treatment. Deprotection of histidine by thiophenol and deformylation of tryptophan by ethanolamine were achieved as recommended by Applied Biosystems. Purification was achieved by preparative reverse-phase HPLC on a 30-nm Vydac C18 column (2.2 × 25 cm, 10 μm). Fractions of the peptide were first loaded onto the column equilibrated with solvent system 1, consisting of 0.1% trifluoroacetic acid and CH_3CN in the ratio 95:5 (v/v), and elution was carried out with a gradient to give a final ratio of 40:60. Further purification was achieved on the same column using a second solvent system containing 0.07% pentafluorophosphoric acid and CH_3CN, using a 30-min linear gradient from 15 to 55% CH_3CN. Desalting of the peptide was obtained by a final chromatographic step using solvent system 1.

CaM Subcloning, Expression, and Purification. CaM clone containing synthetic calmodulin (AF084412; *26*, *27*) was a kind gift of Dr. D. M. Watterson. The open reading frame was subcloned into $pHAT_2$ (*28*) between EcoRI and BamHI sites. *Escherichia coli* BL21(DE3) strain, transformed by the pHAT-CaM construct, was used to overexpress normal or uniformly $^{15}N/^{13}C$-labeled CaM. For labeled CaM, 10 mL of minimal M9-ampicillin medium containing 2 g/L ^{13}C-glucose and 1 g/L $^{15}NH_4Cl$, was inoculated with 100 μL of a saturated culture grown overnight at 37 °C in LB-Amp from a single colony. The culture was then used to inoculate 990 mL of minimal M9-ampicillin medium at 37 °C which was further induced by 1 mM IPTG for 2.5 h at 37 °C after OD600 had reached 0.5. For normal expression, the induction was achieved under the very same conditions, after growing of 1 L LB−Amp first inoculated with 20 to 50 mL of an overnight culture from a single colony, until the OD600 reaches 0.5. After induction of normal or labeled CaM expression, pelleted cells were resuspended in 15 mL of 50 mM Tris pH 8, 100 mM NaCl, 1 mM EDTA, 1 mM DTT, 0.1 mM PMSF, and lysed using French-press. Following centrifugation (18 000 rpm, 30 min at 4 °C) of the sample, the supernatant was cleared by 0.2 μm filtration before $CaCl_2$ was added to a final concentration of 5 mM. Purification to homogeneity was achieved according to Roberts et al. (*27*), using a 15 mL low-sub Phenyl-Sepharose (AP-Biotech) column on a Beckman Biosys2000 FPLC system. After elution with 50 mM Tris pH 7.5, 1 mM EGTA, Apo-CaM was further concentrated and desalted using 5000 Da cutoff centricon (Amicon) and dialyzed against water before freeze-drying. Purity of the samples was monitored by mass spectrometry. Concentrations were measured using OD at 280 nm with a ϵ value of 1580 cm^{-1} M^{-1}. This molar absorption coefficient was estimated from UV−visible spectra after determination of the protein concentration by total amino acid analysis.

CaM C-Terminal Domain Cloning and Overexpression. CaM C-terminal (TR2C) domain clone was a kind gift of Dr. T. Drakenberg (Biophysical Chemistry Department, Lund University, Sweden). The coding sequence was amplified by PCR using conventional methods, with 5′CTGATGGGATCCAAGATGAAAGAC-ACTGA3′ and 5′AGGGCCCTCGAGCCTACTTAGCCATCATAA3′ (MWG-Biotech AG) as primers. The fragment was then subcloned in BamHI and XhoI sites of pGEX4T-3 (AP-Biotech), as a fusion protein with GST. *E. coli* BL21(DE3) strain, transformed by the

above construct, was used to overexpress the recombinant protein in the conditions described above for CaM. After 3 h induction at 37 °C, cells were harvested by centrifugation, and lysed as described above. Purification of TR2C was achieved after loading of the lysis supernatant on 1.5 mL glutathione-Sepharose according to manufacturer's instructions (AP-Biotech). The fusion protein was further purified after direct cleavage by thrombin on the column (50 U, 4 °C). After overnight incubation, remaining thrombin was captured from the eluate by clearing through a 500 μL *p*-amino benzamidine-Sepharose 6B column (Sigma Aldrich). The final eluate, which contained TR2C, was then dialyzed against water and lyophilized. Integrity and purity of the protein were estimated by mass spectrometry.

Dansyl CaM (DNS−CaM) Synthesis. Apo-CaM (20 mg) was dansylated with dansyl-chloride (Sigma Aldrich) as described by Kincaid et al. (*29*). One or two DNS molecules were incorporated per CaM moiety as determined by mass spectrometry; native: *m*/*e*: 18 390 100%; *m*/*e*: 18 622 (+232, 1 dansyl) 83%; *m*/*e*: 18 854 (+464, 2 dansyl) 59%.

Circular Dichroism. Circular dichroism spectra were recorded at 25 °C between 190 and 250 nm on a Jobin-Yvon CD6 spectro-dichrograph, using a quartz cell of 1-mm path length, with a 2 s integration time for each 0.5-nm step. For each experimental condition, two spectra were averaged and corrected from the baseline for buffer solvents.

Fluorescence Emission Spectroscopy. Intrinsic tryptophan emission fluorescence measurements were performed using eithera Bowman 2 Amincon or a Jobin Yvon Spex Fluoro-Max spectrofluorimeter. Unless otherwise specified in the text, experiments were performed in the following conditions: measurements were recorded at room temperature in a 1 × 1 cm cuvette under continuous stirring. The excitation wavelength was set to 295 nm (4 nm band-pass). Emitted light was detected at 90° between 310 and 380 nm (4 nm band-pass). Assays were performed with peptides in the concentration range of 3−10 μM in 20 mM Tris pH 7.7, 1 mM $CaCl_2$. For CaM binding assays, CaM from 0.5 mM stock solution was added stepwise up to a final concentration of 21 μM. For salt-dependence experiments, salts from 4 M stock solutions were added stepwise to peptide/Ca^{2+}-CaM complexes up to a final concentration of 300 mM for NaCl, $NaNO_3$ and KCl or 100 mM for $CaCl_2$, $Ca(NO_3)_2$, and $MgCl_2$. For the TFP-dependence experiments, TFP from 1 mM stock solution was added stepwise up to 25 μM to peptide/Ca^{2+}-CaM complexes formed in the presence of 0.5 mM $CaCl_2$. For the CaM/TR2C competition experiments, CaM (1.3 mM stock solution) or its C-ter domain (1.5 mM stock solution) were added stepwise up to a final concentration of 21 μM to a 5 μM solution of preformed STP23/DNS-CaM complex. The excitation wavelength was set at the maximal excitation wavelength of the DNS-CaM (335 nm, 4 nm band-pass). Emitted light was detected at 90° between 450 and 550 nm (4 nm band-pass). For each experimental point, the intrinsic fluorescence was determined as the difference between the observed fluorescence (F) and the baseline fluorescence determined with an equivalent concentration of NATA (F_{NATA}) under the same conditions, normalized by corrected initial fluorescence ($F_{max} - F_{NATA}$) using the following expression: $(F - F_{NATA})/(F_{max} - F_{NATA})$.

Infrared Spectroscopy. For Fourier transform infrared spectroscopy (FT-IR) studies, the solutions of STP42 and $^{15}N/^{13}C$-labeled CaM were prepared as 0.85 and 0.9 mM solutions, respectively, in a D_2O buffer (20 mM Tris, 5 mM $CaCl_2$, pH 7.7). The complex was obtained by mixing the two latter solutions in a 1/1 ratio. A total of 60 μL of the solutions were inserted between CaF_2 windows (Spectra tech) using a 100 μm spacer. IR spectra were recorded with a JASCO 610 Fourier transform spectrometer. For each spectrum, 1000 interferograms were recorded at 20 °C with a resolution of 4 cm^{-1}. Then, the water vapor was subtracted and the baseline was corrected using the software provided by JASCO (Japan). The spectrum of the peptide bound to CaM was obtained by subtracting the spectrum of the free $^{15}N/^{13}C$-labeled CaM from the spectrum of the complex (peptide/CaM), as described by Zhang et al. (*30*). The spectra of the peptide were normalized using the band of TFA. Then, the second derivatives of the spectra were calculated with the software provided by JASCO.

Nuclear Magnetic Resonance Spectroscopy. A Ca^{2+}-loaded uniformly $^{15}N/^{13}C$-labeled CaM sample was prepared as a 0.7 mM solution in a Shigemi tube (Shigemi Inc., Allison Park, PA) containing 18 mM Tris-base buffer, pH 7.7, 0.05% NaN_3, anti-proteases (Complete, Boehringer, Mannheim) and 10% D_2O. The sample was degassed under argon. The Ca^{2+}-CaM/peptide complex was prepared by direct addition of a concentrated solution of unlabeled STP42 (typically 6 mM) to the NMR sample of labeled Ca^{2+}-CaM to reach a 1:1 stoichiometry. NMR spectra were recorded at 27 °C on Varian Inova 600 and 800 MHz spectrometers equipped with a triple-resonance (^1H, ^{13}C, ^{15}N) probe including shielded z-gradients. To be able to compare the backbone chemical shifts of free and peptide-bound CaM, the backbone chemical shifts of the CaM/peptide complex were assigned under the same conditions as the free CaM. This was done with the following experiments: 2D ^1H-^{15}N HSQC, 3D HNCA, 3D HNCO (*31*−*34*), 3D HN(CO)CA (*35*), and 3D (H)CC(CO)-NH (*36*) spectra. For the HNCA, HN(CO)CA, HNCO, and (H)CC(CO)NH experiments, 1228 × 120 × 58, 1024 × 100 × 55, 1024 × 128 × 52, and 1024 × 70 × 50 (^1H, ^{13}C, ^{15}N) complex points were acquired, respectively. All triple resonance experiments used the pulse sequences provided by the Varian protein pack (available at ftp site: ftp.nmr.varianinc.com). All data were processed using FELIX 2000 (Accelrys). Proton chemical shifts were reported with respect to the H_2O signal relative to DSS at 27 °C. The ^{15}N and ^{13}C chemical shifts were referenced indirectly using the $X/^1H$ frequency ratios of the zero-point: 0.101329118 (^{15}N) and 0.251449530 (^{13}C) (*37*).

RESULTS

Fluorescence Measurements. Initially, we verified whether F-STOP peptide models were able to bind CaM in solution. As illustrated in Figure 1, addition of increasing concentrations of CaM to the STOP peptide STP23 in the presence of 1 mM calcium, induced an increase of the fluorescence intensity and a blue shift of the maximum of reemission of 19 nm. This indicates a more hydrophobic environment in the tryptophan vicinity and demonstrates formation of a complex between Ca^{2+}-CaM and the peptide. Addition of 10 mM EGTA totally reversed the observed changes, indicating that the binding was calcium dependent. The calculated dissociation constant yielded a value of 3.9 ± 1.4 μM, which lies in the range of the published values for CaM/

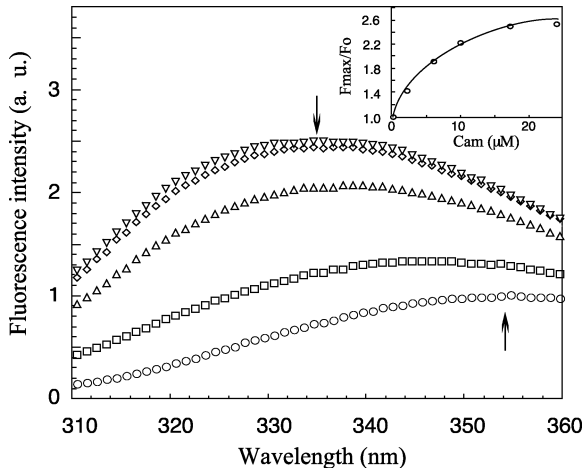

FIGURE 1: Steady-state intrinsic tryptophan fluorescence spectra of STP23 peptide as a function of CaM concentration. 3 μM peptide (open circles); in the presence of 2 μM (open squares), 8 μM (open triangles), 17 μM (open diamonds), and 24 μM CaM (open inverted triangles). Spectra were recorded at 25 °C in the presence of 0.5 mM $CaCl_2$. Excitation was set at 300 nm. The inset shows the evolution of the fluorescence intensity at the maximum emission wavelength as a function of CaM concentration.

F-STOP binding affinities (*16*). Similar results were obtained for the longer peptide corresponding to a single repeat motif (STP42) with a calculated K_d of 5.6 ± 1.2 μM (Supporting Information, Figure S1).

Our result clearly indicates that a single peptide motif binds Ca^{2+}-CaM. We next tested the influence of ionic strength on the binding of CaM to STP23 (Figure 2). Starting from the complex in solution, our data show that an increase in ionic strength leads to a decrease of the fluorescence maximum (Figure 2). The dissociation of the peptide from CaM under increased ionic strength environment is confirmed by a red shift of the λ_{max} toward the value of the unbound form (data not shown), with an almost complete dissociation above 200 mOsm sodium chloride. This is not due to the increase of the chloride concentration, as half-dissociation is obtained only at about 100 mM Cl^- with NaCl, whereas it is quasi-complete at 50 mM Cl^- with $CaCl_2$ (Figure 2A,B). Moreover, we also observed dissociation at similar cation concentrations using nitrate salts instead of chloride salts (Supporting Information, Figure S2). Using STP42 (Supporting Information, Figure S3), we further tested a series of monovalent or divalent ions. Since no specific difference was observed in the dissociation efficiency using sodium or potassium (Figure S3A,C) and calcium or magnesium (Figure S3B,D), we conclude that the nature of the salt used is not responsible for the dissociation observed. We also tested the effect of acidic pH, and observed an increase in dissociation efficiency using divalent ions (data not shown). Taken together our data suggest that CaM interaction with STOP peptides is at least partly electrostatic.

Peptide α*-Helical Content.* Generally, an increase of the α-helical content in the secondary structure of a CaM-binding peptide is induced by the formation of the complex (*38*). This can be observed by CD spectroscopy as an increase of the ellipticity at 208 and 222 nm. Surprisingly, no significant increase of the negative ellipticity took place at 208 and 222 nm when STOP peptides were added, even in the presence of peptide excess (Figure 3A). The only variations we observed in the range of 200−210 nm were due to the intrinsic

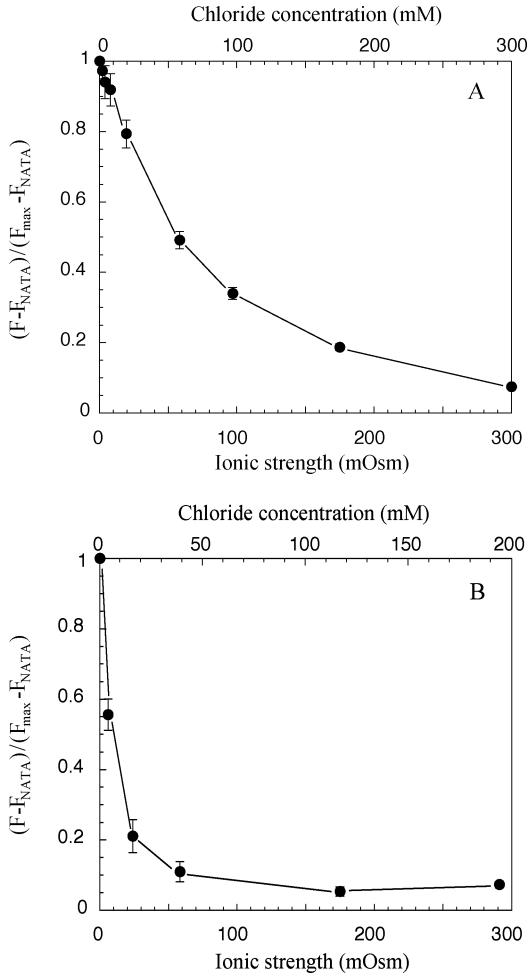

FIGURE 2: Effect of the ionic strength on the STP23/CaM binding. Plotted here is the emitted W-fluorescence, corrected from the NATA-fluorescence recorded in the same conditions and normalized by the complex fluorescence before addition of salts, as a function of the osmolarity: $f = 1/2\ \Sigma(C_i z_i^2)$ where C_i and z_i are the concentration and charge of the i species (lower abscissa) or as a function of the chloride concentration (upper abscissa). Fluorescence was measured for increasing concentrations of NaCl (A) or $CaCl_2$ (B). Spectra were recorded in the presence of 5 μM peptide complexed with 10 μM CaM.

absorption of the peptides (data not shown). We verified by intrinsic W fluorescence using the same samples that, under the conditions used for the CD experiments, binding occurred. The peptides do not adopt a helical conformation by themselves in solution as indicated by a negative ellipticity minimum at 200 nm, nor exhibit a propensity to adopt this conformation, as no significant increase of the helicity was induced by TFE below 15% (data not shown). No spectral variations were observed when 100 mM $CaCl_2$ was added to the peptides, indicating that no structural change takes place in the peptide under these conditions (data not shown). Thus, the ion-dependent inhibition of the binding is not due to a specific folding of the peptides.

To confirm the unusual lack of peptide α-helicity upon binding, we used FTIR spectroscopy to investigate the structure changes induced within STP23 in the presence of CaM. The amide I band, which is due to carbonyl stretching, is particularly valuable for study of the secondary structure of polypeptides. Moreover, by using $^{15}N/^{13}C$-labeled protein it is possible to distinguish the contributions to the FTIR spectrum of the two partners of the complex (*30*, *39*). When

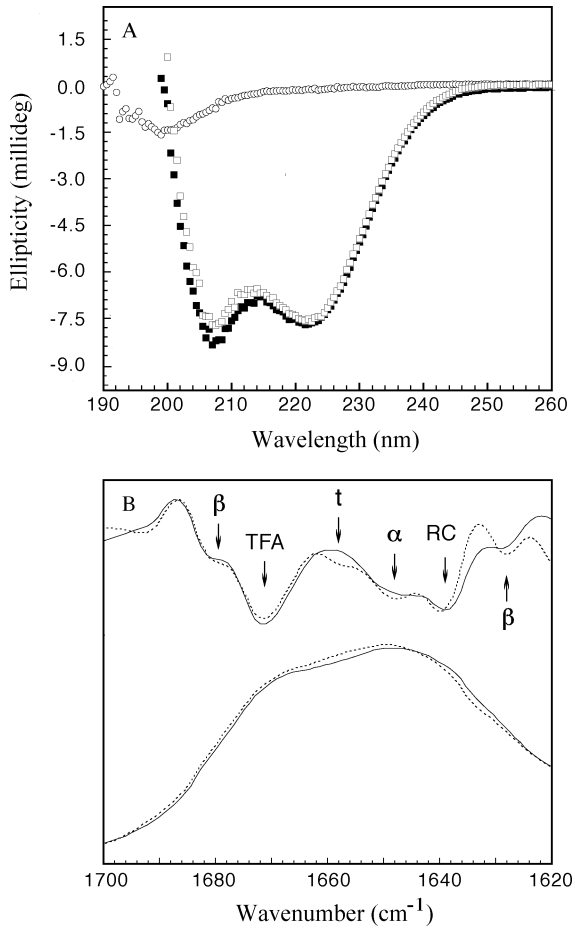

FIGURE 3: (A) Far UV circular dichroism spectra of the STP23/CaM. STP23 alone (open circles); CaM alone (filled squares); STP23/CaM (open squares). Spectra were recorded with 40 μM CaM complexed with a final concentration 40 μM STP23. (B) FTIR spectra of the peptide: effect of the binding to CaM. (Lower panel) Raw spectra of the free peptide (plain line) and the CaM-complexed peptide (dashed line). The spectrum of the peptide bound to CaM was obtained by subtracting the amide I band of the ^{15}N/^{13}C-labeled CaM (see Experimental Procedures). (Top panel) Second derivatives of the raw spectra: free peptide (plain line), CaM-complexed peptide (dashed line). The band assignment is shown on the figure: (β) extended structures; (TFA) TFA; (t) turns; (α) α-helices; (RC) random coil.

^{15}N/^{13}C-labeled CaM is used, its amide I band is shifted (*30*). It is then possible to distinguish the contribution of the bound peptide from that of CaM. In agreement with previous studies (*30*, *40*), the maximum of the amide I band of the unlabeled CaM is at 1644 cm^{-1} (data not shown). The maximum is shifted at 1598 cm^{-1} in the case of the ^{15}N/^{13}C-labeled protein (data not shown). This maximum is not changed when CaM forms a complex with the peptide. Therefore, the spectrum of the peptide bound to CaM can be extracted from the spectrum of the complex by subtracting the spectrum of the free ^{15}N/^{13}C-TR2C, as described by Yuan et al. (*39*).

The maximum of the amide I band in the spectrum of the peptide in solution is at 1646 cm^{-1} (Figure 3B). This maximum is shifted to 1648 cm^{-1} when the protein is bound to CaM. This indicates that the secondary structure of the peptide is modified upon binding to CaM. The second derivative of the spectrum is calculated to distinguish the various components of the amide I band. Aside from a band at 1671 cm^{-1} that is due to residual TFA (used for the peptide synthesis), bands that can be assigned to random coil (1640 cm^{-1}), α-helices (1648 cm^{-1}), and extended structures (1629 and 1680 cm^{-1}) were detected. These extended structures are probably due to a small amount of the peptide, which is aggregated and does not interfere in the binding to CaM. In agreement with the CD spectra, the preponderant band was that of random coil. The band of α-helices was broad as a result of highly fluctuating structures. The main changes detected in the spectrum of the peptide bound to CaM were the narrowing of the bands (except those assigned to extended structures), particularly those of α-helices, and the appearance of a small band at 1658 cm^{-1} that can be assigned to turns (Figure 3B). The sharpening of the band of α-helices suggests that the highly fluctuating α-helical structure in solution is more constrained upon binding to CaM.

NMR Spectroscopy. Despite previous reports of CaM assignments (*31*), complete ab initio reassignment of our CaM sample appeared to be necessary. Slight experimental variations, in particular, the salt concentrations between our conditions and the published ones combined with the primary sequence difference led to chemical shift variations which did not allow unambiguous assignment of the peaks from the published results, in particular, in the central part of the HSQC spectra. Consequently, we performed four 3D experiments (HNCA, HN(CO)CA, HNCO, and (H)C(CCO)NH) which allowed us to assign all the atoms of the backbone protein except the N-terminal His-tag $_1$MSHHHHHHS$_9$. We also obtained 80% of the ^{1}H and ^{13}C chemical shifts of the side chains of the nonaromatic residues. The proton, nitrogen, and carbon chemical shifts of the backbone are reported in Supporting Information (Table S1).

An interaction between proteins is expected to induce structural and dynamic changes, giving raise to chemical shift and line width variations of the signals. The residues of CaM affected by the interaction with the peptide have thus been identified from 2D HSQC spectra. We observed only one CAM species upon addition of aliquots of peptide, indicating that the complex is in a fast exchange regime. Residues were considered to be affected when $[(\Delta^{15}N_{Hz})^2 + (\Delta^1H_{Hz})^2]^{1/2} \geq$ 30 Hz. This value corresponds to twice the experimental resolution at 800 MHz either for the proton ($|\Delta H^N| \geq 0.04$ ppm) or the nitrogen ($|\Delta N| \geq 0.4$ ppm). About two-thirds of the ^{15}N/^{1}H backbone amide chemical shifts remained unaffected by complex formation indicating that the global structure of the domains of CaM was not strongly modified upon complex formation. The assignment was confirmed via a 3D HNCA experiment. The ^{1}H, ^{15}N, and ^{13}Cα chemical shifts of the backbone are reported in Supporting Information (Table S2). Figure 4 shows the major variations induced on the H^N and amide ^{15}N chemical shifts by the addition of STP42 to a Ca^{2+}-CaM solution. Surprisingly, the major changes are located in the C-terminal domain. The affected residues in the C-terminal domain are about twice as many as those in the N-terminal domain (see legend to Figure 4), and the main chemical shift changes are principally located in the C-terminal domain of CaM. Interestingly, among residues exhibiting large variations are hydrophobic residues that show nOe contacts with the peptide in the CaM/M13 (*41*) or CaM/CaMKK (*42*) complexes. This suggests that hydrophobic interactions may play an important role in the CaM/STP42 binding. The secondary structure of the complex was estimated from the differences between the experimental and the random coil Cα chemical shifts (ΔCα). These ΔCα

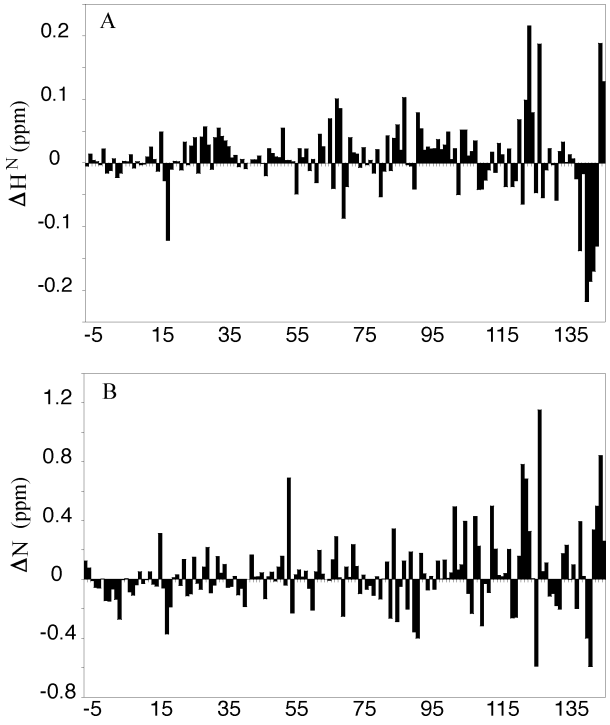

FIGURE 4: Variations of the ^{1}H and ^{15}N chemical shifts of CaM on complex formation. The STP42 peptide was at a final molar ratio of 1/1 Ca^{2+}-CaM/peptide. The difference of the chemical shifts observed in the ^{15}N-HSQC spectra is displayed as a function of the sequence number. Residues were considered to be affected when $[(\Delta^{15}N_{Hz})^2 + (\Delta^{1}H_{Hz})^2]^{1/2} \geq 30$ Hz. This value corresponds to twice the experimental resolution at 800 MHz either for the proton ($|\Delta H^N| \geq 0.04$ ppm) or the nitrogen ($|\geq N| \geq 0.4$ ppm). The 18 residues affected in the N-terminal domain are S17, F19, I27, T29, K30, GTV33−35, N53, V55, A57, D64, EFLNL67−71, A73. The 32 residues affected in the C-terminal domain are E82, E84, E87, F89, FDK92−94, A102, ELRH104−107, TNL110−112, K115, EMIRE-ADV123−130, G134, F141, QVMMAK143−148.

shifts indicate that the secondary structures of the N- and C-terminal domains are basically the same as for free CaM and the CaM/M13 complex (data not shown). This result strongly suggests, as for the other peptide complexes, that the two domains do not change their tertiary backbone structure upon binding to the peptide. ΔCα values for the central region of the protein are presented on Figure 5. Surprisingly, we did not observe any significant change in the central region of CaM corresponding to the α-helix connecting the N-terminal and C-terminal domains. This strongly suggests that the central helix is not disrupted in the binding in contrast to classical CaM/peptide complexes (*43*) and that CaM retains an open conformation in our case. This observation could be related to our finding that most residues affected upon binding are located in the C-terminal region of the protein, indicating that the peptide binds mainly to this domain in a manner which may not require central helix disruption (as illustrated in Figure 6).

The Peptide Binds to CaM C-Terminal Domain. To further analyze the nature of the CaM/STOP interaction, and to confirm the implication of the CaM C-terminal domain in STOP peptide binding, we tested the effect of trifluoroperazine (TFP) on binding characteristics. TFP is a classical inhibitor of CaM-dependent activation of its effectors through direct interaction with CaM. TFP binding is complex, but involves mostly the C-terminal CaM subdomain (*44*). Using

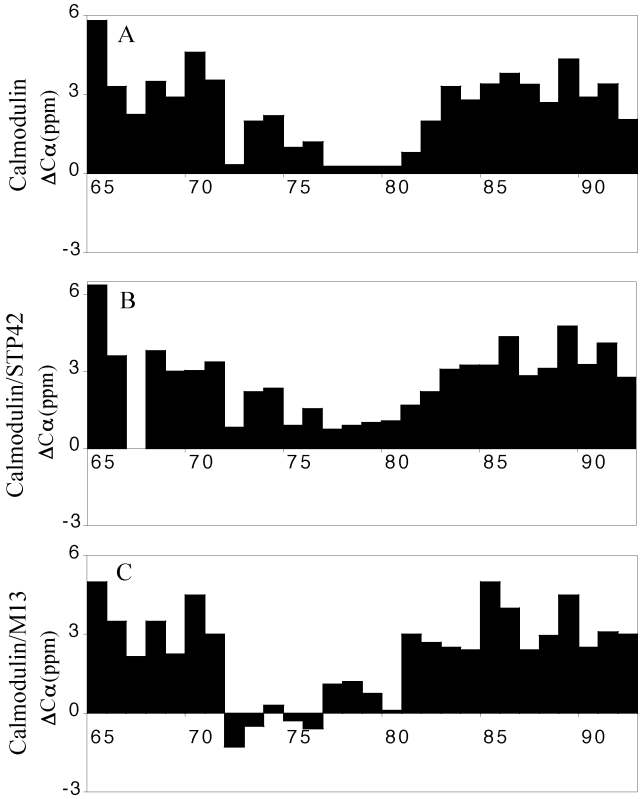

FIGURE 5: The differences between the experimental and the random coil Cα chemical shifts (ΔCα) of free CaM (A), the CaM/STP42 complex (B), and the CaM/M13 complex (C) for the central helix. Here the ΔCα shifts of the free CaM (A) and the CaM/STP42 complex (B) closely follow each other while those of the CaM/M13 complex (C) are significantly different.

CD spectroscopy as described by Vertessy et al. (*45*), we first measured TFP affinity for our CaM sequence (data not shown), and obtained a constant in the range of 1−2 μM, as expected from published data (*45*, *46*). As shown in Figure 7A, the addition of TFP led to a large decrease of the maximal fluorescence associated with a red shift of the maximum toward the λ_{max} value of the free peptide. This indicates that TFP inhibits peptide binding and suggests that the Mc motif competes with TFP for the same binding site, which comprises the hydrophobic pocket in the C-terminal domain.

To further investigate the mode of interaction of CaM with the peptide, we then performed competition experiments between CaM and its C-terminal domain (TR2C). As illustrated in Figure 7B, TR2C displaced dansylated-CaM (DNS-CaM) from STOP peptide with an efficiency similar to that of wild-type CaM. These convergent data strongly suggest that CaM-binding modules of F-STOP interact predominantly with CaM C-terminal domain, whereas the N-terminal domain has only an accessory role in STOP binding.

DISCUSSION

In this work, we have characterized the interaction between Ca^{2+}-CaM and peptide models corresponding to the Mc motif of the repeated microtubule-binding domain of F-STOP protein. We demonstrate that peptide binding to Ca^{2+}-CaM is unusual, mostly involving its C-terminal domain, and implicating to some extent electrostatic interactions. Moreover, NMR spectra analyses strongly suggest that CaM remains in an extended conformation.

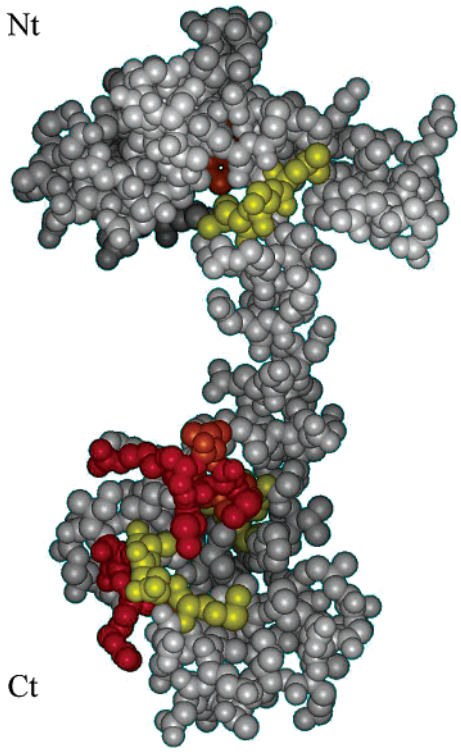

FIGURE 6: Spatial distribution of the chemical shift variations observed between CaM and the CaM complexed with STP42 at a molar ratio of 1/1 Ca^{2+}-CaM/peptide. The variations are mapped onto the crystallographic structure of free *P. tetraurelia* Ca^{2+}-CaM (*59*). Major variations are observed in the C-terminal domain. Yellow, orange, and red indicate the locations of amino acids whose $[(\Delta^{15}N_{Hz})^2 + (\Delta^{1}H_{Hz})^2]^{1/2}$ were between 60 and 90 Hz (L69, N70, L71, F89, D93, M124, E127, A128), between 90 and 120 Hz (F19, I125, F141, M146, K148), and over 120 Hz (R126, D129, Q143, V144, M145, A147), respectively.

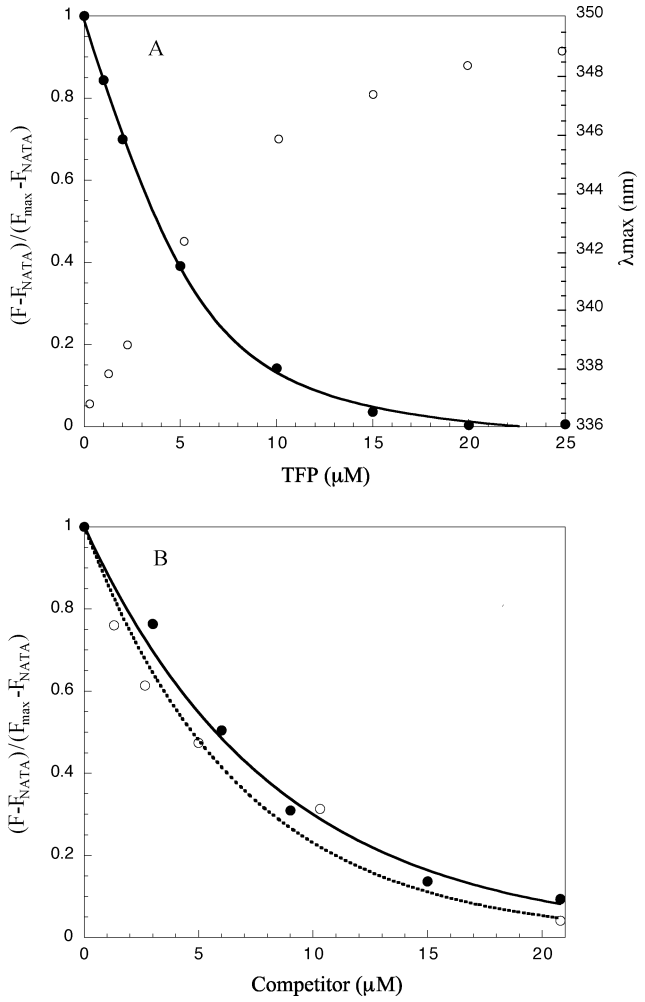

FIGURE 7: (A) Effect of TFP on CaM binding to STP23. The W-fluorescence corrected from the NATA fluorescence, recorded in the same conditions and normalized by the initial steady-state complex fluorescence (filled circles), and the emission wavelength at the maximum of each fluorescence spectrum (open circles) were expressed as a function of the TFP concentration. Spectra were recorded in the presence of 10 μM peptide complexed with 10 μM CaM. Excitation was set at 290 nm to avoid interference with TFP fluorescence. Reemitted fluorescence signals were integrated 20 nm around the maximum of each individual emission spectrum. (B) Competition between integral CaM and its C-terminal domain for STP23 binding. The DNS fluorescence corrected from the NATA fluorescence, recorded in the same conditions and normalized by the initial steady-state complex fluorescence, was expressed as a function of the competitor concentration: CaM (open circles) and TR2C (filled circles). Spectra were recorded in the presence of 0.5 mM $CaCl_2$ for a concentration of 6 μM peptide complexed with 5 μM DNS-CaM. Output signals were integrated between 450 and 550 nm.

Previously reported data showed that at least a tandem repeat of the Mc motif was required for proper CaM-Agarose binding (*16*), suggesting that two Mc motifs might bind a single CaM molecule. To our knowledge, a 2:1 peptide to CaM binding stoichiometry has been only reported for the complex formed between CaM and the carboxy-terminal domain of the Petunia glutamate decarboxylase (*18*). An even more complex situation has been described for the phosphorylase kinase, where one CaM interacts with two distinct peptides of its gamma subunit (*19*). Structures of two complexes where CaM binds to more than a single peptide have been determined, in complex with the edema factor of *Bacillus anthraxis* (*20*), or with the gating-domain of a Ca^{2+}-activated K^+ channel (*21*). In our hands, however, 2D ^{15}N-HSQC spectra in the presence of 1:1 and 2:1 peptide versus CaM ratios show equivalent variations of the ^{1}H and ^{15}N chemical shifts when compared to Ca^{2+}-CaM alone (data not shown). It is thus highly probable that the weak binding of a single Mc motif to immobilized CaM described in published work (*16*) is related to the experimental conditions used, i.e., 100 mM NaCl. We indeed clearly demonstrate here that Mc binding is very sensitive to ionic strength, as is native F-STOP binding (unpublished results), decreasing association efficiency by 70% in the presence of 100 mOsm NaCl (Figures 2A and S3A). In their published study (*16*), Bosc et al. suggest, from Scatchard plots, that F-STOP bears two types of CaM-binding sites: low affinity and high affinity. However, this hypothesis does not correlate with the presence of both Mc and Mn CaM binding motifs, since only Mc repeats in F-STOP bind immobilized Ca^{2+}-CaM (*16*). Thus, we cannot exclude the possibility that STOP binding to CaM through repeated Mc motifs is cooperative, suggesting that F-STOP might undergo a global structural rearrangement upon CaM binding.

Generally, complexes formed between specific peptides and Ca^{2+}-CaM share typical features: (i) high affinity binding in the 10−100 nM range; (ii) sensitivity to hydrophobic inhibitors such as TFP or W-7; (iii) essentially hydrophobic interaction due to contacts between methionines of CaM and aromatic or bulky hydrophobic residues of the peptide which is thus insensitive to high ionic strength; and

(iv) from the structural point of view, wrapping of the two CaM subdomains around the peptide which in turn adopts an α-helical conformation (*10*, *47*, *48*). The complex we have characterized between CaM and a single Mc motif of F-STOP repeated region exhibits very unusual features, which contrast with the classical model. Although the binding is calcium dependent, the affinity is low, in the micromolar range, more similar to that observed for calcium-independent binding domains (*10*, *47*, *48*). Second, the binding is very sensitive to ionic strength, which also contrasts with most of the other peptide binding motifs. Such a property suggests a mainly ionic interaction between the negatively charged amino acids of CaM and the basic residues of the peptide. In our case, although the exact location of the binding zone in the peptide cannot be precisely determined as yet, the sequence corresponding to the Mc motif exhibits a high proportion, about 60%, of basic and polar residues. Moreover, CD spectra (Figure 3A) indicate that the binding of the peptide to CaM has no effect on the overall α-helical structure in the complex. The possibility of a loss of CaM structure, compensated by gain of peptide structure induced by binding can be ruled out by our NMR results which show only slight variations of the CaM chemical shifts, in particular, the $^{13}C\alpha$ chemical shifts which are highly dependent on the structure. This analysis is corroborated by infrared spectroscopy, which does not indicate any significant structural change in CaM, while the signals associated with the peptide are clearly perturbed. These convergent results indicate that Mc peptide motif binds CaM without adopting the canonical α-helical conformation, in contrast to typical hydrophobic CaM-binding peptides. To date, in three-dimensional structures of peptides in complex with Ca^{2+}-CaM, the interacting peptide is found to adopt an α-helical conformation upon binding (*21*, *41*, *42*, *49*−*53*).

In complex with the Mc motif peptide, Ca^{2+}-CaM appears to retain a conformation similar to that of free Ca^{2+}-CaM (Figure 5). In the usual cases described to date, the wrapping of Ca^{2+}-CaM around the bound peptide is indeed accompanied by a disruption of the central α-helix connecting the two subdomains (*43*). This conformational transition induces very typical changes of the Cα chemical shifts in the interdomain α-helix of Ca^{2+}-CaM (*43*). Moreover, we clearly demonstrate both by NMR and direct competition assays that the Mc motif peptide of STOP interacts mainly with the C-terminal part of CaM (Figures 6 and 7). Indeed, chemical mapping indicates that the most affected region upon peptide binding is the C-terminal half of CaM (cf. Figure 4), suggesting the N-terminal half of CaM has only an accessory role (if any) in the binding. Interestingly, we demonstrate that the binding of the STP23 Mc motif peptide to Ca^{2+}-CaM is inhibited by TFP with an IC_{50} of about 4 μM (Figure 7A), which suggests a competition for the same site between the two species. This is further supported by the published mapping of the C-terminal binding site of TFP on Ca^{2+}-CaM, where 9 residues out of 13 having contacts with TFP in CaM/TFP complex (*44*) are also involved in Mc peptide binding (F92, L105, E123, M124, I125, E127, A128, F141, V144). Our data suggest that competition with TFP could be at least partly the result of steric hindrance.

These very atypical features for Ca^{2+}-CaM/peptide complexes have been observed in two other cases: CaM-binding domains of the SEF2-1/E12 protein and the MARCKS and MARCKS-related proteins. Binding inhibition has been reported in both cases for model-peptide binding to Ca^{2+}-CaM above 25 mM $CaCl_2$ for MARCKS, and 200 mM NaCl for SEF2-1/E12 (*22*, *54*), i.e., comparable to what we observe for the Mc motif studied here. In both cases, the peptides bear very high content in basic amino acids (50%) and low content in hydrophobic amino acids when compared to typical CaM-binding domains, a property which has been related to the observed salt sensitivity (*22*, *54*). In the formed complexes, the peptides have been also reported to bind to Ca^{2+}-CaM without acquiring any α-helical conformation as determined by CD spectroscopy for the MARCKS CaM-binding domain (*24*, *54*), the F52/MARCKS-related CaM-binding domain (*25*, *54*), the Ral-A protein (*55*) and by NMR for the SEF2-1mp domain (*23*). In the latter case, absence of chemical shift variations between free Ca^{2+}-CaM and Ca^{2+}-CaM/peptide complexes has been observed, suggesting an extended conformation of Ca^{2+}-CaM in solution (*23*). Such an extended conformation for complexed Ca^{2+}-CaM has been also proposed for the basic CAP-23/NAP22 CaM-binding domain using SAXS spectroscopy (*23*, *56*). Functionally, a preferential interaction with the C-terminal domain of CaM has been reported for the bHLH protein E12, which exhibits a basic domain analogous to SEF2-1mp (*22*). Thus, the recently reported structure of the CaM/MARCKS peptide complex could give interesting insights into the interaction mode of Ca^{2+}-CaM/Mc motif binding. Indeed, the MARCKS peptide is found to take an elongated structure, with only a short one-turn α-helix surrounded by two loops (*57*). Such a conformation would be, for our peptide, in agreement with the CD and IR results, which indicate only the stabilization upon CaM binding of a preexisting fluctuating α-helical structure in solution. MARCKS peptide also binds to Ca^{2+}-CaM through interaction of a single hydrophobic residue with the hydrophobic pocket of the C-terminal lobe of CaM. This role could be mimicked in the Mc module by the tryptophan. Unfortunately, we have not been able yet to assign the peptides within the complex and consequently to determine either the CaM-binding region or the Mc motif conformation in the bound state. These points are under investigation using a labeled-peptide sample.

MARCKS peptide interacts with the N-terminal lobe of CaM in crystals, leading it to wrap around the peptide, with a disruption of CaM central α-helix (*57*). This is a major difference with the conformation of CaM in complex with the F-STOP Mc motif. First, major contacts between N-terminal domain and the MARCKS peptide are observed for CaM residues 10−15, a zone that is unaffected in our complex. Second, we do not observe any significant change for the central helix, suggesting an open conformation of CaM similar to that observed in free Ca^{2+}-CaM. In this species, the tumbling of the two domains remains independent, as described in the "flexible tether" model (*58*). Thus, we suggest that in the CaM/STP-peptide complex, the chemical shift variations we observed in the N-terminal lobe of CaM are related to its temporary interaction with the C-terminal lobe of the complex. In the MARCKS complex, wrapping of CaM might still be the consequence of the steric constraint imposed by crystal stacking. Even though previous NMR results have been interpreted as due to the disruption of the central helix and a closed CaM conformation (*25*), it is notable that data are missing for residues in the CaM

central α-helix, leaving open the possibility of a restrained flexibility rather than true wrapping around the peptide.

Our results reinforce the recent views on CaM binding modes, pointing out that Ca^{2+}-CaM interacts with its targets with more variety than previously imagined (*59*). Nonglobular wrapping of bound CaM has been described in complexes formed with Ca^{2+}-activated K^+ channel and Anthrax edema factor (*20*, *21*). This is also illustrated in the complex formed between the C20W peptide of the plasma membrane calcium pump and the C-terminal lobe of Ca^{2+}-CaM (*60*). Ca^{2+}-CaM interaction with STOP-Mc motif involves mainly its C-terminal lobe, leaves CaM in an extended conformation, and potentially permits interaction of its N-terminal domain with another partner. This intriguing possibility remains to be investigated.

Physiological CaM-binding to F-STOP may represent an even more unusual complex formation. Mc motifs are repeated in the central domain of cloned STOP proteins, raising the possibility that several Ca^{2+}-CaM interact with a single STOP under physiological conditions. Interestingly, homology searches in EST databases for STOP-related proteins in different organisms have shown that Mc motif is not always repeated, and may even be absent (*16*). As mentioned above, F-STOP colocalizes with CaM at the microtubule spindle during mitosis (*11*). The measured K_d of Ca^{2+}-CaM for Mc motif is in the micromolar range. Such an affinity rules out the possibility that microtubule associated F-STOP is responsible for the specific relocalization of CaM during mitosis. On the other hand, their colocalization may lead to specific interaction of F-STOP and CaM in the close vicinity of the spindle. In fact, microtubule dynamics are a key to mitotic progression (*61*). CaM is also known to be required for proper progression through mitosis (*14*, *15*). The fact that CaM is the only known regulator of microtubule stabilization by STOP suggests that their interaction may have a physiological function during mitosis. It will be of interest to know how the unusual CaM binding to STOP may be implicated in this process.

ACKNOWLEDGMENT

We thank J. P. Andrieu (LEM-IBS) for amino acid analyses, LSMP-IBS for mass spectrometry analyses, L. Blanchoin for technical assistance, and E. Denarier and C. Bosc for helpful reagents. D.B. and C.V. were recipients of a CEA fellowship.

SUPPORTING INFORMATION AVAILABLE

Steady-state intrinsic tryptophan fluorescence spectra of STP42 peptide as a function of CaM concentration (Figure S1), effect of nitrate salts on STP23/CaM binding (Figure S2), and effect of the ionic strength on the STP42/CaM binding (Figure S3). Proton, nitrogen-15, and carbon-13 chemical shift assignment of Ca^{2+}-calmodulin backbone atoms (Table S1) and STP42-complexed Ca^{2+}-calmodulin backbone atoms (Table S2). This material is available free of charge via the Internet at http://pubs.acs.org.

REFERENCES

1. Chapin, S., and Bulinski, J. (1992) Microtubule stabilization by assembly promoting microtubule-associated proteins: a repeat performance. *Cell Motil. Cytoskeleton 23*, 236−243.
2. Margolis, R. L., Rauch, C. T., and Job, D. (1986) Purification and assay of a 145-kDa protein (STOP145) with microtubule-stabilizing and motility behavior. *Proc. Natl. Acad. Sci. U.S.A. 83*, 639−643.
3. Pabion, M., Job, D., and Margolis, R. L. (1984) Sliding of STOP proteins on microtubules. *Biochemistry 23*, 6642−6648.
4. Bosc, C., Cronk, J. D., Pirollet, F., Watterson, M. D., Haiech, J., Job, D., and Margolis, R. L. (1996) Cloning, expression, and properties of the microtubule-stabilizing protein STOP. *Proc. Natl. Acad. Sci. U.S.A. 93*, 2125−2130.
5. Denarier, E., Fourest-Lieuvin, A., Bosc, C., Pirollet, F., Chapel, A., Margolis, R. L., and Job, D. (1998) Nonneuronal isoforms of STOP protein are responsible for microtubule cold stability in mammalian fibroblasts. *Proc. Natl. Acad. Sci. U.S.A. 95*, 6055−6060.
6. Guillaud, L., Bosc, C., Fourest-Lieuvin, A., Denarier, E., Pirollet, F., Lafanechere, L., and Job, D. (1998) STOP proteins are responsible for the high degree of microtubule stabilization observed in neuronal cells. *J. Cell Biol. 142*, 167−179.
7. Andrieux, A., Salin, P. A., Vernet, M., Kujala, P., Baratier, J., Gory-Faure, S., Bosc, C., Pointu, H., Proietto, D., Schweitzer, A., Denarier, E., Klumperman, J., and Job, D. (2002) The suppression of brain cold-stable microtubules in mice induces synaptic defects associated with neuroleptic-sensitive behavioral disorders. *Genes Dev. 16*, 2350−2364.
8. Pirollet, F., Derancourt, J., Haiech, J., Job, D., and Margolis, R. L. (1992) Ca(2+)-calmodulin regulated effectors of microtubule stability in bovine brain. *Biochemistry 31*, 8849−8855.
9. Pirollet, F., Margolis, R., and Job, D. (1992) Ca(2+)-calmodulin regulated effectors of microtubule stability in neuronal tissues. *Biochim. Biophys. Acta 1160*, 113−119.
10. Chin, D., and Means, A. R. (2000) Calmodulin: a prototypical calcium sensor. *Trends Cell Biol. 10*, 322−328.
11. Li, C. J., Heim, R., Lu, P., Pu, Y., Tsien, R. Y., and Chang, D. C. (1999) Dynamic redistribution of calmodulin in HeLa cells during cell division as revealed by a GFP-calmodulin fusion protein technique. *J. Cell Sci. 112 (Pt 10)*, 1567−1577.
12. Erent, M., Pagakis, S., Browne, J. P., and Bayley, P. (1999) Association of calmodulin with cytoskeletal structures at different stages of HeLa cell division, visualized by a calmodulin-EGFP fusion protein. *Mol. Cell Biol. Res. Commun. 1*, 209−215.
13. Moser, M. J., Flory, M. R., and Davis, T. N. (1997) Calmodulin localizes to the spindle pole body of *Schizosaccharomyces pombe* and performs an essential function in chromosome segregation. *J. Cell Sci. 110 (Pt 15)*, 1805−1812.
14. Rasmussen, C. D., and Means, A. R. (1989) Calmodulin is required for cell-cycle progression during G1 and mitosis. *EMBO J. 8*, 73−82.
15. Torok, K., Wilding, M., Groigno, L., Patel, R., and Whitaker, M. (1998) Imaging the spatial dynamics of calmodulin activation during mitosis, *Curr. Biol. 8*, 692−699.
16. Bosc, C., Frank, R., Denarier, E., Ronjat, M., Schweitzer, A., Wehland, J., and Job, D. (2001) Identification of novel bifunctional calmodulin-binding and microtubule- stabilizing motifs in STOP proteins. *J. Biol. Chem. 276*, 30904−30913.
17. Choi, J. Y., Lee, S. H., Park, C. Y., Heo, W. D., Kim, J. C., Kim, M. C., Chung, W. S., Moon, B. C., Cheong, Y. H., Kim, C. Y., Yoo, J. H., Koo, J. C., Ok, H. M., Chi, S. W., Ryu, S. E., Lee, S. Y., Lim, C. O., and Cho, M. J. (2002) Identification of calmodulin isoform-specific binding peptides from a phage-displayed random 22-mer peptide library. *J. Biol. Chem. 277*, 21630−21638.
18. Yuan, T., and Vogel, H. J. (1998) Calcium-calmodulin-induced dimerization of the carboxyl-terminal domain from petunia glutamate decarboxylase. A novel calmodulin-peptide interaction motif. *J. Biol. Chem. 273*, 30328−30335.
19. Dasgupta, M., Honeycutt, T., and Blumenthal, D. K. (1989) The gamma-subunit of skeletal muscle phosphorylase kinase contains two noncontiguous domains that act in concert to bind calmodulin. *J. Biol. Chem. 264*, 17156−17163.
20. Drum, C. L., Yan, S. Z., Bard, J., Shen, Y. Q., Lu, D., Soelaiman, S., Grabarek, Z., Bohm, A., and Tang, W. J. (2002) Structural basis for the activation of anthrax adenylyl cyclase exotoxin by calmodulin. *Nature 415*, 396−402.
21. Schumacher, M. A., Rivard, A. F., Bachinger, H. P., and Adelman, J. P. (2001) Structure of the gating domain of a Ca2+-activated K+ channel complexed with Ca2+/calmodulin. *Nature 410*, 1120−1124.

22. Onions, J., Hermann, S., and Grundstrom, T. (2000) A novel type of calmodulin interaction in the inhibition of basic helix-loop-helix transcription factors. *Biochemistry 39*, 4366−4374.
23. Larsson, G., Schleucher, J., Onions, J., Hermann, S., Grundstrom, T., and Wijmenga, S. S. (2001) A novel target recognition revealed by calmodulin in complex with the basic helix−loop−helix transcription factor SEF2−1/E2−2. *Protein Sci. 10*, 169−186.
24. Matsubara, M., Yamauchi, E., Hayashi, N., and Taniguchi, H. (1998) MARCKS, a major protein kinase C substrate, assumes nonhelical conformations both in solution and in complex with Ca2+-calmodulin. *FEBS Lett. 421*, 203−207.
25. Porumb, T., Crivici, A., Blackshear, P. J., and Ikura, M. (1997) Calcium binding and conformational properties of calmodulin complexed with peptides derived from myristoylated alanine-rich C kinase substrate (MARCKS) and MARCKS-related protein (MRP). *Eur. Biophys. J. 25*, 239−247.
26. Haiech, J., Kilhoffer, M. C., Craig, T. A., Lukas, T. J., Wilson, E., Guerra-Santos, L., and Watterson, D. M. (1990) Mutant analysis approaches to understanding calcium signal transduction through calmodulin and calmodulin regulated enzymes. *Adv. Exp. Med. Biol. 269*, 43−56.
27. Roberts, D. M., Crea, R., Malecha, M., Alvarado-Urbina, G., Chiarello, R. H., and Watterson, D. M. (1985) Chemical synthesis and expression of a calmodulin gene designed for site-specific mutagenesis. *Biochemistry 24*, 5090−5098.
28. Peranen, J., Rikkonen, M., Hyvonen, M., and Kaariainen, L. (1996) T7 vectors with modified T7lac promoter for expression of proteins in *Escherichia coli*. *Anal. Biochem. 236*, 371−373.
29. Kincaid, R. L., Billingsley, M. L., and Vaughan, M. (1988) Preparation of fluorescent, cross-linking, and biotinylated calmodulin derivatives and their use in studies of calmodulin-activated phosphodiesterase and protein phosphatase. *Methods Enzymol. 159*, 605−626.
30. Zhang, M., Fabian, H., Mantsch, H. H., and Vogel, H. J. (1994) Isotope-edited Fourier transform infrared spectroscopy studies of calmodulin's interaction with its target peptides. *Biochemistry 33*, 10883−10888.
31. Ikura, M., Kay, L. E., and Bax, A. (1990) A novel approach for sequential assignment of 1H, 13C, and 15N spectra of proteins: heteronuclear triple-resonance three-dimensional NMR spectroscopy. Application to calmodulin. *Biochemistry 29*, 4659−4667.
32. Grzesiek, S., and Bax, A. (1992) Improved 3D triple-resonance NMR techniques applied to a 31 kDa protein. *J. Magn. Reson. 96*, 432−440.
33. Muhandiram, D. R., and Kay, L. E. (1994) Gradient-enhanced triple-resonance three-dimensional NMR experiments with improved sensitivity. *J. Magn. Reson. B103*, 203-216.
34. Kay, L. E., Xu, G. Y., and Yamazaki, T. (1994) Enhanced-sensitivity triple-resonance spectroscopy with minimal H_2O saturation. *J. Magn. Reson. A109*, 129−133.
35. Yamazaki, T., Lee, W., Arrowsmith, C. H., Muhandiram, D. R., and Kay, L. E. (1994) A suite of triple resonance NMR experiments for the backbone assignment of ^{15}N, ^{13}C, ^{2}H labeled proteins with high sensitivity, *J. Am. Chem. Soc. 116*, 11655−11666.
36. Grzesiek, S., Anglister, J., and Bax, A. (1993) Correlation of backbone amide and aliphatic side-chain resonances in $^{13}C/^{15}N$-enriched proteins by isotropic mixing of ^{13}C magnetization. *J. Magn. Reson. B101*, 114−119.
37. Wishart, D. S., Bigam, C. G., Yao, J., Abildgaard, F., Dyson, H. J., Oldfield, E., Markley, J. L., and Sykes, B. D. (1995) 1H, 13C and 15N chemical shift referencing in biomolecular NMR. *J. Biomol. NMR 6*, 135−140.
38. Fasman, G. D. (1996) *Circular Dichroism and the Conformational Analysis of Biomolecules*, Plenum Press, New York.
39. Yuan, T., Walsh, M. P., Sutherland, C., Fabian, H., and Vogel, H. J. (1999) Calcium-dependent and -independent interactions of the calmodulin-binding domain of cyclic nucleotide phosphodiesterase with calmodulin. *Biochemistry 38*, 1446−1455.
40. Krueger, J. K., Gallagher, S. C., Wang, C. A., and Trewhella, J. (2000) Calmodulin remains extended upon binding to smooth muscle caldesmon: a combined small-angle scattering and Fourier transform infrared spectroscopy study. *Biochemistry 39*, 3979−3987.
41. Ikura, M., Clore, G. M., Gronenborn, A. M., Zhu, G., Klee, C. B., and Bax, A. (1992) Solution structure of a calmodulin-target peptide complex by multidimensional NMR. *Science 256*, 632−638.
42. Osawa, M., Tokumitsu, H., Swindells, M. B., Kurihara, H., Orita, M., Shibanuma, T., Furuya, T., and Ikura, M. (1999) A novel target recognition revealed by calmodulin in complex with Ca^{2+}-calmodulin-dependent kinase kinase. *Nat. Struct. Biol. 6*, 819−824.
43. Ikura, M., Kay, L. E., Krinks, M., and Bax, A. (1991) Triple-resonance multidimensional NMR study of calmodulin complexed with the binding domain of skeletal muscle myosin light-chain kinase: indication of a conformational change in the central helix. *Biochemistry 30*, 5498−5504.
44. Cook, W. J., Walter, L. J., and Walter, M. R. (1994) Drug binding by calmodulin: crystal structure of a calmodulin-trifluoperazine complex. *Biochemistry 33*, 15259−15265.
45. Vertessy, B. G., Harmat, V., Bocskei, Z., Naray-Szabo, G., Orosz, F., and Ovadi, J. (1998) Simultaneous binding of drugs with different chemical structures to Ca2+-calmodulin: crystallographic and spectroscopic studies. *Biochemistry 37*, 15300−15310.
46. Levin, R. M., and Weiss, B. (1977) Binding of trifluoperazine to the calcium-dependent activator of cyclic nucleotide phosphodiesterase. *Mol. Pharmacol. 13*, 690−697.
47. Crivici, A., and Ikura, M. (1995) Molecular and structural basis of target recognition by calmodulin. *Annu. Rev. Biophys. Biomol. Struct. 24*, 85−116.
48. Rhoads, A. R., and Friedberg, F. (1997) Sequence motifs for calmodulin recognition. *FASEB J. 11*, 331−340.
49. Meador, W. E., Means, A. R., and Quiocho, F. A. (1992) Target enzyme recognition by calmodulin: 2.4 A structure of a calmodulin-peptide complex. *Science 257*, 1251−1255.
50. Meador, W. E., Means, A. R., and Quiocho, F. A. (1993) Modulation of calmodulin plasticity in molecular recognition on the basis of X-ray structures. *Science 262*, 1718−1721.
51. Mirzoeva, S., Weigand, S., Lukas, T. J., Shuvalova, L., Anderson, W. F., and Watterson, D. M. (1999) Analysis of the functional coupling between Calmodulin's calcium binding and peptide recognition properties. *Biochemistry 38*, 14117−14118.
52. Wall, M. E., Clarage, J. B., and Phillips, G. N. (1997) Motions of calmodulin characterized using both Bragg and diffuse X-ray scattering. *Structure 5*, 1599−1612.
53. Kurokawa, H., Osawa, M., Kurihara, H., Katayama, N., Tokumitsu, H., Swindells, M. B., Kainosho, M., and Ikura, M. (2001) Target-induced conformational adaptation of calmodulin revealed by the crystal structure of a complex with nematode Ca(2+)/calmodulin-dependent kinase kinase peptide. *J. Mol. Biol. 312*, 59−68.
54. Schleiff, E., Schmitz, A., McIlhinney, R. A., Manenti, S., and Vergeres, G. (1996) Myristoylation does not modulate the properties of MARCKS-related protein (MRP) in solution. *J. Biol. Chem. 271*, 26794−26802.
55. Wang, K. L., Khan, M. T., and Roufogalis, B. D. (1997) Identification and characterization of a calmodulin-binding domain in Ral-A, a Ras-related GTP-binding protein purified from human erythrocyte membrane. *J. Biol. Chem. 272*, 16002−16009.
56. Hayashi, N., Izumi, Y., Titani, K., and Matsushima, N. (2000) The binding of myristoylated N-terminal nonapeptide from neuro-specific protein CAP-23/NAP-22 to calmodulin does not induce the globular structure observed for the calmodulin-nonmyristylated peptide complex. *Protein Sci. 9*, 1905−1913.
57. Yamauchi, E., Nakatsu, T., Matsubara, M., Kato, H., and Taniguchi, H. (2003) Crystal structure of a MARCKS peptide containing the calmodulin-binding domain in complex with Ca-(2+)-calmodulin. *Nat. Struct. Biol. 10*, 226−231.
58. Barbato, G., Ikura, M., Kay, L. E., Pastor, R. W., and Bax, A. (1992) Backbone dynamics of calmodulin studied by 15N relaxation using inverse detected two-dimensional NMR spectroscopy: the central helix is flexible. *Biochemistry 31*, 5269−5278.
59. Vetter, S. W., and Leclerc, E. (2003) Novel aspects of calmodulin target recognition and activation. *Eur. J. Biochem. 270*, 404−414.
60. Elshorst, B., Hennig, M., Forsterling, H., Diener, A., Maurer, M., Schulte, P., Schwalbe, H., Griesinger, C., Krebs, J., Schmid, H., Vorherr, T., and Carafoli, E. (1999) NMR solution structure of a complex of calmodulin with a binding peptide of the Ca2+ pump. *Biochemistry 38*, 12320−12332.
61. Andersen, S. S. (2000) Spindle assembly and the art of regulating microtubule dynamics by MAPs and Stathmin/Op18. *Trends Cell Biol. 10*, 261−267.

BI034746W